REVIEW

Indian J. Phys. **69A** (5), 477–500 (1995)

IJP A
- an international journal

Growth and behaviour of iron monolayers

G S N Reddy and V S Tomar*
National Physical Laboratory, Krishnan Road, New Delhi-110 012, India

Received 3 April 1995, accepted 14 April 1995

Abstract : Growth of monolayers is a profound subject in itself. Here, we review the growth of iron monolayers on copper and other single crystal substrates. The properties of these films are different from other metals. We discuss the important electrical, magnetic and surface structural behaviour.

Keywords : Transition metals, superlattices, epitaxy

PACS Nos. : 74.70 Tx, 68.55 Gi, 74 80.Dm

Plan of the Article

1. Introduction

Ultrathin films of metals on single crystal substrates have been useful in studying magnetic properties of two dimensional systems. In this film form these properties are very different from their bulk counter parts. In order to grow these films, physics of interaction of

* Author to whom all correspondence should be addressed.

substrate and surface atoms, nucleation and interface properties and the epitaxial character of the metallic grown film are the vital factors. Theoretically, these interactions are described in terms of Lenard-Jones Potentials (LJP) for these and for other subsequent overlayers. In this review, our aim is to study growth of Fe ultra thin films on simple substrates such as copper, gold and gallium arsenide and to summarise their electrical, magnetic and structural characteristics.

2. Metallic monolayers and their special features

2.1. Misfit dislocations in ultra thin metallic films :

Lattice misfit or mismatch at the interface between the substrate and deposited film influences the epitaxial growth. Misfit Dislocations (MDs) can be found in partially coherent epitaxial layered structures. Figure 1 shows comparative atomic arrangement in two cases *viz.* ideal and partially coherent cases. In general, the formation of MDs in ultra-thin metallic films depends upon (i) whether or not, the thin film is elastically strained (*i.e.* pseudomorphic) and at what stage the elastic strain is relieved by MD and (ii) the mode of growth *i.e.* monolayer growth or nucleated growth.

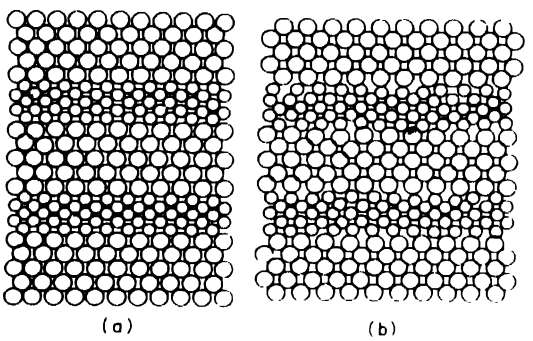

Figure 1. Schematic drawings of (a) coherent, and (b) partially coherent layered structures In the coherent structure the planes perpendicular to the substrate are of constant spacing and alternating layers are under tension and compression In the partially coherent structure the strains are relieved by the introduction of misfit dislocations [Mc Whan (1985)]

During the growth of either Volmer-Weber (VW) mode or Stranski-Krestanow (SK) mode, misfit dislocations can form during the initial stage of nucleation simply by the local distribution of the misfit at the interface as shown in the Figure 2. In this case with increase in the lateral size of the nuclei, one observes that the MD network extends with the interface. Once a continuous film is deposited, it forms a continuous MD network, although the coalescence of nuclei result in irregular network coupled with formation of threading dislocations. The percentage of misfit is simply defined as in $m = 100\ (b - a)/a$, where a is the spacing of atoms (or ions) rows in the substrate surface and b is the equivalent spacing in the parallel rows in the thin films. The epitaxy only occurs when the misfit is less than ~15%. Extensive observations have shown that a small misfit is no more a necessary

requirement for epitaxy [1]. For some of the MDs no evidence could be found [2] in comparison to the growth of tin on tin telluride [3,4].

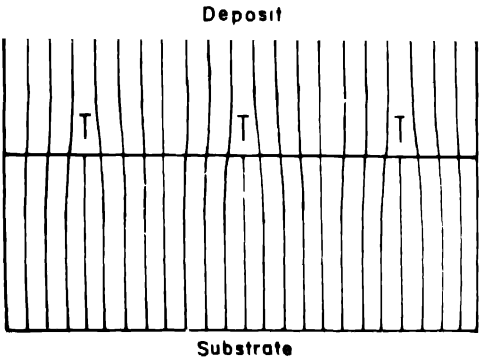

Figure 2. The formation of misfit dislocations between the substrate and the epitaxy deposit to accommodate the misfit between the two deposits

2.2 Strains in the films :

The strains usually exist in epitaxial thin films where the pseudomorphic layers are formed. Oriented thin films are strained elastically so that their lattice spacings match those of the substrate at the interface between them. This strain is accompanied by strain of the opposite sign normal to the interface, so as to maintain a nearly constant atomic volume. If relaxation of pseudomorphic elastic strain occurs before the 3D nucleation stage commences the introduction of misfit dislocations should follow the mechanisms of FM monolayer growth (Figure 3).

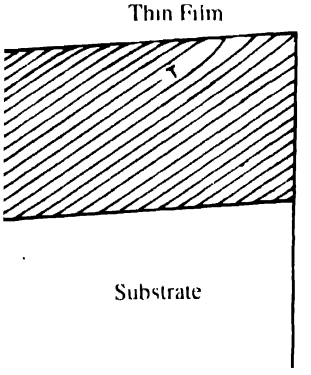

Figure 3. The relief of compressive pseudomorphic strain by nucleation of a dislocation loop, which expands by climb, to produce misfit dislocation at the interface

It is suggested that thickening of the thin film by successive growth of monolayers would lead to relaxation of the elastic strain and the formation of edge dislocations at the

substrate/thin film interface. A good example of the determination of lattice constant T_c for a metallic system is that of gold grown on (111) palladium surfaces [5]. The result, with pseudomorphism extending only for the first two monolayers, to give a T_c value of about 0.45 nm, followed by the gradual relief of the pseudomorphic strain during the growth of the next eight monolayers. This strain relief is understood to arise due to gradual formation of misfit dislocations.

2.3. Pseudomorphism :

The first proposal that pseudomorphism could occur during epitaxy is made by Finch and Quarrell [6(a)]. The proposed pseudomorphic aluminium is shown [1,7] to be based upon a misinterpretation of diffraction patterns, and Newman [8] had cast serious doubts on the Cochrane [9] evidence for pseudomorphic nickel and cobalt. Thus the concept of pseudomorphic layers, theoretically attractive though it was, had to remain a somewhat speculative concept, with no conclusive experimental support. No direct proof of the existence of pseudomorphism, is observed with the High Energy Electron Diffraction (HEED) evidence, because pseudomorphism occurs under conditions unfavourable for the HEED and Reflected High Energy Electron Diffraction (RHEED) observations.

2.3.1. Epitaxy :

Frank and van der Merwe [10] introduced the idea that the growth of an epitaxial thin film depends upon the initial growth of a monolayer of the thin film, which is strained elastically to match (*i.e.* have zero misfit with) the substrate surface. This is based upon the concept of pseudomorphism introduced by Finch and Quarrell [6], where oriented thin films are strained elastically so that their lattice spacing match those of the substrate at the interface betwen them. This strain is accompanied by strain of the opposite sign normal to the interface, so as to maintain a nearly constant volume This idea has proved to be correct for many substrate/thin film combinations studied during the last 25 years. The way in which these dislocations accommodate the misfit between the substrate and the thin film is illustrated in Figure 2. This idea is incorporated into the classic theoretical treatment of Frank and van der Merwe [10] in which the effect of the magnitude to the misfit on the formation of pseudomorphic monolayers is considered. It is that such monolayers would form for misfit below a certain limiting value in the region 10-15% An equally important advance resulted from attempts to calculate the expected lattice strains (*i.e.* degree of pseudomorphism) under different conditions. Such calculations by van der Merwe [11] and Jesser and Kuhbmann-Wils-dorf [12] predicted the limits of pseudomorphism is in remarkably close agreement with the experimentally observed limits.

2.4. Orientations :

Monolayer growth of a metallic film over a crystalline surface may have misfit dislocations and strains in the layers. These are reflected in the oriented growth of the film. This is decided by matching of the substrate and the film material as well (a) isomorphic case

where lattices of film and substrate are nearly identical and (b) nonisomorphic case where only atomic configuration resemble when lattices are dissimilar.

In multilayer growth case, first layer of the film tries to exactly imitate the substrate surface. Subsequent monolayers however, try to match the first layer. Matching of the film grown depends on orientation of the substrate surface. For example, as shown in the Table 1

Table 1. Epitaxial orientations of metals on MgO [13]

Metal	Orientations			Ratio
	(110)	(001)	(111)	R
Ni	strong	less	—	0.84
Cu	strong	less	—	0.85
Pd	—	strong	—	0.92
Pt	—	strong	less	0.93
Al	—	strong	—	0.96
Fe	—	strong	—	0.96
Au	—	—	strong	0.97
Ag	—	strong	—	0.97

[13], nickel monolayer will have strong oriented growth on (110) oriented substrate and have lesser on (001) and have no probability on the (111) oriented substrate. For example, the *bcc* Fe (110) on Ag domains are grown [14] in stated Nishiyama-Washerman (NW) orientation, Fe on Pd(111) [14(b)] Kurdiimo-Sacks (KS) orientation.

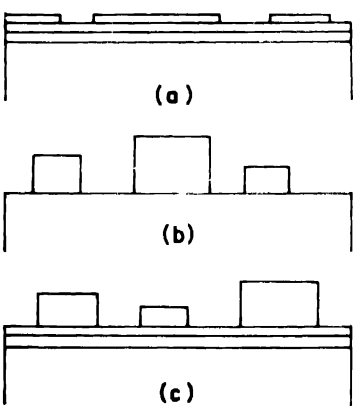

Figure 4. The modes of growth of epitaxial layers (a) The Frank and vander Merwe (FM) monolayers 2D mode, (b) The Volmer-Weber (3D) mode, (c) The Stranki-Krastanow (SK) mode involving monolayer 2D growth followed by 3D growth.

2.5. *Monolayer deposition :*

The initial stages of growth can be classified into 3 idealized kinds of nucleation. The three distinct nucleation modes of growth are illustrated in Figure 4 [14(a), 15]. Figure 4(a)

consists of monolayer or two dimensional growth. Figure 4(b) growth mode involves initial formation of a surface distribution of 3D nuclei, separated by uncovered region of the substrate surface. Whether 2D or 3D growth occurs, initially it can be considered in terms of surface energies. Rapid increase of strain energy resulting in an instability of the multilayer with respect to formation of MDs is favourable to SK growth as shown in Figure 4(c) [16]. Thin crystalline films grow near equilibrium by one of three mechanisms, Volmer-Weber (VW), Stanski-Krestanow (SK) and Frank and van der Merwe (FM) modes, depending upon the relative magnitude of the surface energies in the following equation. For all n (dependent strain energy *i.e.* independent of thickness)

$$\Delta\Gamma_n = \Gamma_{fn} + \Gamma_{in} + \Gamma_s < 0, \tag{1}$$

where Γ_{fn} = surface energy of the thin film, Γ_{in} = the interfacial energy, Γ_s = the surface energy of the substrate and n being the number of monolayers.

2.5.1. FM growth :

The first growth mode follows from the theory of Frank and van der Merwe [10(a)], hence it is called the FM growth mode monolayer mode. It consists of monolayers or two dimensional growth (2D). The thin film grows monolayer by monolayer. The lattice mismatch is however, neither necessary nor sufficient for FM growth. For this growth mode to occur rather the condition (2) has to be fulfilled [8,16]. Monolayer by monolayer growth occurs only in this FM mode with $\Gamma_{fn} \cong \Gamma_s$; $\Gamma_{in} = 0$ or it is very small in comparison with Γ_s and Γ_{fn} homoepitaxy *i.e.* zero misfit. If strain contribution Γ_{fn} to Γ_{in} is zero and

$$\Gamma_{fn} \quad \Gamma_{in} - \Gamma_s > 0, \tag{2}$$

here Γ_{fn} is zero strain contribution to Γ_{in}, which depends on the specific chemical interaction between film and substrate atoms and rapidly approaches zero within the first few monolayers, depending upon the range of the interatomic forces.

The first monolayer of transition metals is strongly influenced by chemical surface modifications such as oxygen or carbon adsorption [14(b)]. This causes rapid increase of the strain energy (Em) resulting in an instability of multilayer with respect to the formation of misfit dislocations and the development of conditions favourable to SK growth for n as small as 2 or 3. Even if SK growth prevails under quasi-eqilibrium, pseudo FM growth can be obtained at a sufficiently low temperature, which in many cases is the room temperature. This shows that even when $\Gamma_{fn} << \Gamma_s$ so that $\Delta\Gamma_n < 0$ is true initially, pseudo FM growth conditions are necessary in order to obtain films with low roughness.

2.5.2. VW growth .

Figure 4(b) shows Volmer-Weber (VW) deposition mode. The second growth mode involves the initial formation of a surface distribution of 3D (three dimensional) nuclei, separated by uncovered regions of the substrate surface. The size and number of these 3-dimensional nuclei change as further deposition continues, until the nuclei coalesce and

eventually form a continuous thin film. This mode is normally known as the Volmer-Weber (VW) mode of growth.

Here $$\Delta\Gamma_n = \Gamma_{fn} + \Gamma_{in} - \Gamma_s < 0 \qquad \text{for } n = 1. \tag{3}$$

Considerable efforts, both experimental and theoretical have been devoted to the understanding of the kinetics of nucleation in the VW mode. So far in the literature [17,18], the interest has centered upon topics such as (i) the smallest size of stable cluster, which would determine the initial nuclei, (ii) the rate of formation of stable nuclei for given deposition conditions, (iii) the geometrical distribution of nuclei over the substrate surface and (iv) the change in size and number of nuclei as deposition continues, particularly to take account of the onset of the coalescence of nuclei leading to a reduction in numbers.

Some attempts also have been made to determine the most energetically favourable orientations of a small stable nucleus on a single crystal, with the hope that this could provide a means of developing a theory of epitaxy which could predict, which orientations will occur in a given situation. The best known treatment is that of Walton [19] whose approach helped to explain the orientation of *fcc* metals on alkali halides, even though the misfit values are very high (27%) it has not resulted in the prediction of orientations in many other systems. For this reason, no further consideration is given to the nucleation kinetics.

2.5.3. SK growth :

The third mode of growth is the combination of the other two. 2D growth occurs first, but after few monolayers have formed, the mechanism changes and the 3D nuclei form on the upper most layer. Further growth then occurs as for the Volmer Weber mode. This third mode is known as the (SK) Stanski-Krestanow mode.

In all other cases, the increase of the strain energy with n leads to an increase of Γ_{in} until at a given $n = n^*$ (n maximum) *i.e.* the FM condition is not fulfilled any longer and 3D crystal from. This is called SK mode,

here $$\Delta\Gamma_n = \Gamma_{in} + \Gamma_{im} - \Gamma_s > 0. \tag{4}$$

Baur and Poppa [14(a)] identified the SK mode as intermediate between the other two modes FM and VW. Various examples of SK mode have been observed. There are now an increasing number of reports concerning epitaxial metal thin films [18,20] Much of the earlier evidence is based upon the inferences drawn from Auger electron spectroscopy. The Auger signal originates from only the top few atom layers of a surface. The monolayer growth causes the signal from the substrate to be reduced strongly for growth of just a few monolayers, shown in Figure 5(b). For 3D nucleation, the Auger signal from the substrate remains strong for relatively large amounts of deposit Figure 5(a). The intermediate SK mode causes the Auger signals to change as shown in Figure 5(c).

The scanning electron microscope in conjunction with Auger electron spectroscopy and RHEED [21] have also been used to provide direct evidence of the SK mode [22] applicable to *in situ* deposition.

3. Growth of ultrathin iron films

In our above discussion we had discussed growth, microstructure and orientation of metal films in general, which are fabricated using molecular beam epitaxy methods. In order to have more specific understanding, we are concentrating fully on taking up Fe monolayers as an example. Such knowledge is very important for modern multilayer device development.

Fe is a ferromagnetic (transition) metal with $Z = 26$ and $A = 52$. It has its M-shell incompletely filled and thus contains only 14 electrons instead of 18. Out of which 9 electrons have their spin in clockwise while five in anticlockwise directions. The uncompensated 4 electrons produce a magnetic field at a distance equal to 4 electrons. Therefore, Fe has a magnetic moment of 4 units. Thus, ferromagnetism in iron originates from the unfilled M-shells in Fe atoms. Experimentally measured value of the magnetic moment of Fe is 2.22 units and is lower compared to the isolated free atoms.

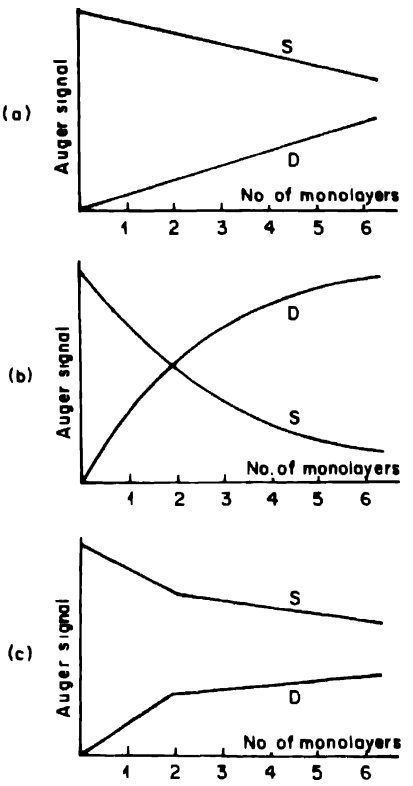

Figure 5. The effect of different modes of growth on the Auger signal from the surface during AES analysis : (a) 3 dimensional nucleation according to VW mode; (b) monolayer growth, (c) SK growth with 3 dimensional nucleation acquiring after the formation of two monolayers (S = substrate, D = deposited thin film).

In absence of applied magnetic field, Fe atomic magnets point in one direction. The internal magnetic field required to bring order to the atomic magnets for their alignment

towards one direction is called a Weiss molecular field. In case of Fe, its intensity is 5.5×10^6 A/cm.

The force of interaction in such atoms is a function of the ratio of the distance (D) between the neighbouring atoms and the diameter of the atomic shell (d) responsible for the atomic magnetic moments. It is a strong ferromagnetic material because the ratio D/d is larger than 1.5. When the temperature is increased to a certain value called Curie temperature, the ferromagnetic material transforms into a paramagnetic state. The Curie temperature of Fe is 770°C, where thermal vibrations of the atoms become stronger and the atomic magnets orient themselves randomly. Advances in sample preparation and characterisation techniques for ultrathin Fe films and superlattices have led to the discovery of many exciting new phenomena in the last decade [23]. The surface anisotropy, gaint magnetoresistance and magnetic couplings in multilayers are some of them.

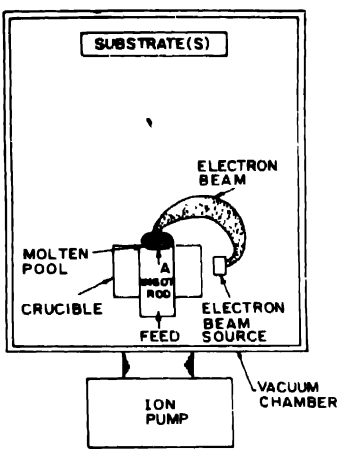

Figure 6. Schematics of internal source configuration of the MBE system deposition process for epitaxial Fe films.

The successful application of MBE technology in the preparation of semiconductor superlattices has led to the observation of a variety of properties of several materials [24]. Some of these properties such as enhanced electron mobility in modulation doped superlattices, have found application in electron devices. Similarly, the growth and exploration of transition metal superlattices is expected to reveal a range of modified transport properties resulting from the chemical modulation. For example, we can have superlattice modification of Fermi surface topology. Such expectations have led to preparation of metal superlattices, culminating in the recent success in preparation of Nb-Ta superlattices [25].

Thin film deposition in general, is made in an MBE system equipped with electron beam sources. Since these metals can have a gettering action with residual gases, it is necessary to reduce the ambient pressure to ~ 10^{-9} torr during deposition. The base pressure

is kept around 2×10^{-10} torr. This is achieved in MBE systems. A typical system is shown in Figure 6.

A variety of superlattices have been prepared using sputtering techniques [26]. These techniques do not yield metastable phases. This limitations of vapour growth technique is believed to occur due to following factors [27-30].

(i) These methods can all form phases at much lower temperatures than is possible by growing from the melt.

(ii) The introduction of impurities into the forming material is likely to occur. Moreover, the impurities such as carbonitrides are more stable than the nitrides [28].

(iii) Sputtering and evaporation in particular, are often considered to be very high rate quenching methods by which equilibrium phases can be 'frozen in' at lower temperature.

(iv) High vacuum apparatus maintains critical pressure < 10^{-10} torr [29].

This particular research application of metallization by MBE appears very fertile since the technique has great flexibility and potential in engineering the film anisotropy properties. For example, the addition of Si to Fe should have the effect of reducing the mismatch strain and also the resulting misfit dislocation density. Interestingly the *fcc* compound Fe_3Si should have a near perfect interface registry to GaAs since $a(Fe_3Si) = (1/2)$ a(GaAs) with in 0.1%. A significant improvement in structural perfection of the Fe films can also be expected from predeposition of either a GaAs or Ge buffer layer. Epitaxial overgrowth of lattice matched fluoride films [31] for passivation is also possible.

However, pseudomorphic growth of Fe on different single crystal substrates is difficult to obtain because the surface free energy of Fe (2.939) J-m^{-2} is significantly larger than the free energies of single crystal substrates given in Table 2. For Fe films grown on Cu and Ag substrates do not fulfill the condition $\Delta\Gamma < 0$ irrespective of surface orientation, because Γ_{Fe} = 2.94 J-m^{-2} is larger than the Γ_{Cu} = 1.93 J-m^{-2} and Γ_{Ag} = 1.3 J-m^{-2} [32]. It is also known from film morphology that the transition of *fcc* Fe(111) to *bcc* Fe(110) on Cu(111) is due to the balance between intrafilm interaction strength and the film substrate interaction strength [33] and the initial phases of room temperature heteroepitaxy of *fcc* Fe/Cu(100) indicate that vertical atomic site exchange occurs locally during the deposition of first two monolayers [34].

The films deposited at low temperature 80 K show evolution of a *bcc* Fe phase, which is consistent with nearly layer-by-layer growth on Cu(111) [35]. Some more examples of ideal layer-by-layer growth are Fe, Co and Cu on Cu(100) at 80 K [36]. This growth mode is in contrast to most of the reports [37-40], which indicate room temperature FM growth of Fe/Cu(111). The effect of varying substrate temperature between 80 K and 450 K plays a prominent role in determining both the film morphology and crystalline phase as shown in Table 2 [41-46]. Layer-by-layer growth should not be expected in many

other metastable film-substrate systems. Growth of Fe monolayer on Cu(100) results from intermixing of arriving atoms with the top layer of the substrate [47].

Table 2. Growth conditions of Fe superlattice on different substrates.

Metallic phase	Growth temp (K)	Vacuum (Torr)	Lattice mismatch (%)	Substrates	Ref
fcc Fe (111)	80–450	2×10^{-10}	-0.8	Cu (111)	[41]
fcc Fe (100)	80	2×10^{-10}	1.1	Cu (100)	
bcc Fe (110)	80	2×10^{-10}	3.4	Cu (111)	
bcc Fe (110)	80	2×10^{-10}	10.6	Cu (100)	
bcc Fe (100)	80	2×10^{-10}	---	Cu (100)	[42]
fcc Fe (110)	80	2×10^{-10}	---	Cu (110)	
fcc Fe (100)	100–300	1×10^{-11}	---	Cu (100)	[43]
bcc Fe (100)	100–300	1×10^{-11}	0.6	Au (100)	
bcc Fe (100)	100–300	1×10^{-11}	0.6	Au (100)	[44]
bcc Fe	273	2×10^{-10}	1.24	GaAs (110)	[45]
fcc Fe (111)	100–300	1×10^{-11}	5.5	Ru (0001)	[43]
fcc Fe (100)	273	4×10^{-10}	1.1	Ag (100)	[46]
bcc Fe (100)	273	4×10^{-10}	14	Ag (100)	

GaAs is a semiconducting material. It is listed for comparison sake

The element Cu has a face centered cubic structure with a lattice parameter at 18°C of 3.615 Å. The phase (body centered cubic structure) of the element Fe which is thermodynamically stable phase upto $T = 916$°C has a lattice parameter at 18°C of 2.855 Å. Thus, an interface between Cu and Fe formed near room temperatures would be expected to contain a very large number of interfacial misfit dislocations since the numerical value of the misfit is $100(b - a)/a \sim 20.7\%$ and no symmetric periodic registry between the structures (as can be obtained for Al or Ag on GaAs by rotation of the film lattice) is possible on the other hand the *b*-phase of Fe, which is thermodynamically stable only over a limited temperature range (916-1400°C) has a lattice parameter, extrapolated to 18°C, of 3.591 Å, which represents a misfit to Cu of only $(b - a)/a = -7 \times 10^{-3}$. Jesser and Matthews [48] found that room temperature deposition of Fe on the (001) surface of Cu in UHV has resulted in 2D pseudomorphic growth of the γ-phase of iron up to a thickness of ~ 20 Å. No misfit dislocations are detected in the γ-Fe film until its thickness exceeded 20 Å.

During room temperature growth of Fe monolayers on a Au(001), the atomic place exchange of Au atoms is observed in the angular profile measurement of High Resolution

Low Energy Electron Diffraction (HRLEED) experiment [44]. Thermal stability and atomic intermixing of ultrathin ferromagnetic Fe films grown on Au(001) surface have been studied using HRLEED [44,49]. The submonolayer heteroepitaxial Fe film of thickness ~ 500 Å deposited on a Au(001) substrate at ~ 1200 K in UHV chamber [49] exhibits the place exchanged atoms result in 2D Au surface islands and Fe subsurface structures In thicker films, misfit dislocations, Moire fringes, and nuclei of Fe are observed, indicating the onset of relaxation of the metastable film to its thermodynamically stable state by generation of local disorder. This phenomenon of stabilization of the γ-phase of Fe by epitaxy is striking and has opened up the prospect for preparation of a variety of interesting and potentially useful metastable phases of other materials by a similar technique.

MBE technique have been applied to the preparation of epitaxial films of Fe on GaAs in order to explore, for the first time, the magnetic properties of single crystal Fe films. Prinz and Krebs [50] used a Knudsen effusion source containing Fe at ~ 1150°C (in a pyrolytic boron nitride crucible) to generate a low-intensity beam of Fe for growth of thin (< 200 Å) films on GaAs at ~ 3.3 A min^{-1} in an MBE system. Recently, many authors used this technique to fabricate Fe films on different substrates as listed in Table 2. The thermodynamically stable phase of Fe formed upto 916°C, has a lattice parameter within 1.4% of a factor of 2 smaller than GaAs, that is a (Fe) = 2.866 Å compared with (1/2) × *a*(GaAs) = 2.827 Å at 25°C. The *b*(*fcc*) phase of Fe, which nucleates [48,20] as a metastable phase on (fcc) Cu at room temperature, has a lattice parameter of 3.59 Å and is therefore, not expected to nucleate on GaAs at low (< 450°C) temperatures. Parallel (unrotated) epitaxy of Fe on (110) GaAs is to be expected because of close registry of Fe atoms with As (or Ga) atoms along (100) and (001) directions. This epitaxial relation is confirmed by Prinz and Krebs [50] who selected the (110) surface of GaAs for epitaxy so that the three major directions (110), (111) and (001) of the Fe crystal were in the film plane. This permitted a full exploration of the magnetic anisotropy of the Fe films.

Pseudomorphic growth of Fe on Ag(100) is slightly expanded because there is a 0.8% mismatch between the γ-Fe(100) and Ag(100) surface nets [51]. Furthermore, Fe and Ag have very little overlap of the valance electron bands [52,53] leading to only a small degree of band hybridization and thus, permitting the approximate realization of quasi two dimensional Fe thin films with enhanced magnetic anisotropy relative to bulk Fe.

In the first series of experiments [25(b)], the metals are deposited on to (1120) sapphire substrates held at 700-900°C. It is also found that the structural perfection of the superlattice is highest for the (1120) oriented sapphire crystals. Since coherent growth for metals with bulk lattice mismatches of ~ 1% extends [12] typically over > 20Å, the choice of metals could be widened at the expense of introducing strain anisotropy into the superlattices.

In general, the quasiequilibrium FM, VW and SK growth modes do not adequately describe the growth kinetics of the Fe/Co and Co/Cu systems. Simple considerations of surface diffusion and surface free energies provide basis for understanding the observed growth modes. The surface energies of various substances have been listed in Table 3 by

Table 3. Surface energies for oriented substrates

Surface	Face	Surface energy ($nJ\text{-}nm^{-2}$)
Cu	(111)	2554
Cu	(100)	2932
γ-Fe	(110)	3032
γ-Fe	(100)	4010
Ni	(111)	3246
Ni	(100)	3720
W	(110)	3000
MgO	(100)	1200
KBr	(100)	137
KCl	(100)	152
NaCl	(100)	170
$CaCO_3$	(1010)	230
LiF	(100)	340
CaF_2	(111)	450
Cd	(0001)	62

Kern *et al* [20]. It is reasonable to expect that other meta-stable metal-film/metal-substrate systems [54] should also necessitate a more dynamic description than provided by FM, VW and SK growth modes.

4. Surface science studies

Electron diffraction technique is one of the standard surface science methods for studying surface structure of thin films. The modern technique such as Reflected High Energy Electron Diffraction (RHEED) arrangement is well adopted for diffraction work and therefore, used as the standard electron diffraction device in this field.

Because of the large scattering cross section of matter for electrons, electron diffraction is ideally suited for the study of thin films. Since interference maxima occur at angles $\theta = D/2$, where D = diffraction angle or Laue angle, according to Bragg's equation $2d \sin \theta = n \lambda$, the diffraction cone $2D$ is restricted to about 6, permitting the use of flat films or plates for the recording of the diffraction patterns. Similar to microscopy, a

monochramatic electron beam is being used exclusively in RHEED and Low Energy Electron Diffraction (LEED) analysis.

4.1. Leed :

The growth structure of Fe films on Cu (111) have been studied using Electron Microscopy (EM) [48,55], field ion microscopy [56] and LEED [40,57-59] and Scanning Tunneling Microscopy (STM) study for Fe/Cu(100) [60]. Here LEED patterns for Fe films show a gradual transition in structure with increasing thickness at room temperature. The LEED pattern observed for 8 ML of Fe grown at 300 K is compared to the LEED patterns for KS and NW orientations In the experimental LEED pattern, the alignment is predominantly KS and demonstrated the presence of multiple *bcc* domains originating in the six equivalent orientations. Similar LEED patterns have been observed for KS orientations of *bcc* Fe on (*hcp*) hexagonal-close-packed Ru(0001) [61]. Fe film growth temperatures between 80 and 300 K has profound effects upon the film morphology and crystallographic structure for Fe on Cu(111). Fe deposited on Cu(111) at substrate temperature of 80 K grows *bcc* and Fe deposited at a substrate temperature of 300 K initially grows *fcc* and relaxes to *bcc* with increasing thickness [40,57]. LEED measurements show that the Fe is strained to match the Cu lattice pseudomorphically. Fe tends to agglomerate more strongly at the higher temperature. In addition the surface segregation of the Cu becomes more prominent with increasing substrate growth temperature. Fe film morphology in terms of surface diffusion and agglomeration, which increase with temperature Pure agglomeration suggests formation of 4 ML thick clusters.

LEED patterns for Fe deposited on Cu(110) show streaks and splitting along the furrowed (110) direction. The structure is expected for diffusion along the furrows and occurs even at 80 K [35]. At higher coverages of Fe on Cu(100), the oscillations damp out as an added material reverts to the bulk *bcc* Fe structure. This is indicated by LEED as an outcome of the ordering of the overlayers [62]. Thermal stabilities and atomic intermixing of ultrathin ferromagnetic Fe films grown on a Au (001) surface have been studied using high resolution LEED [44,49]. Both the average size and the average inhomogeneity length can be quantitatively determined as a function of temperature by properly decomposing the energy dependent angular profiles of the (00) beam measured from Fe/Au(001) films at various temperatures and the distribution of exchanged atoms in submonolayer heteroepitaxial film Fe/Au(001) is also observed using angular profile measurement of high resolution LEED [44,49].

4.2. Rheed :

The crucial distinction between no mobility and low mobility is demonstrated by the presence of RHEED oscillations even at 80 K, well below temperatures where thermal diffusion is expected for Fe/Cu(100) [63]. It has been shown that there are no RHEED oscillations for purely random deposition with no mobility, relaxing the constraints to allow random deposition at (100) fourfold hollow sites can induce oscillation, while maintaining

random statistics in the first layer [60]. RHEED patterns on Fe(001)/Cu(001) indicate that the system require a 12.5% distortion to match *fcc* Cu to *bcc* Fe, whereas metastable phases of epitaxial *bcc* Cu(001) overlayers were grown on *bcc* Fe(001) [64]. The decay of the Fe/Cu(100) specular beam RHEED oscillations [63] marks the departure from the *fcc* phase after 10 ML. Simultaneously, they observe symmetric splitting in the RHEED spots off the [65] azimuth. Similar decays in the oscillations have been recently reported in 3 KeV (100) RHEED oscillations between 12 and 15 ML with streaks developing along the (110) directions in both RHEED and LEED [62,66]. The re-entrant behaviour of the first RHEED maximum with growth temperature is an important clue to the Fe on Cu (100) growth dynamics [35].

The higher temperature growth appears aided by surface segregation of the Au, which acts to reduce the surface free energy and promotes a more complicated layer-by-layer growth. This phenomenon has been suggested for Fe/Au(100) system through RHEED observations [67]. Recent RHEED investigation on the MBE growth of Fe/Cr/Fe-layered system, reveal interfacial reconstruction and show that the surface is smoothed out by the electron beem bombardment [68].

5. Electrical and magnetic properties

The majority of metallic multilayers have been used in research on many interesting properties such as electron transport, magnetic or magneto-optic data storage *etc* and many possibilities remain to be explored. Although electron transport phenomena in metallic multilayers are of great scientific interest, they seem unlikely to be the basis of large scale commercial applications for example, semiconductor multilayers. It is too early still for multilayer studies, however, to identify the main future applications, especially in the light of the wide range of special properties.

Iron has been an important ferromagnetic material since ages. Superlattices of iron have been interesting for observation of magnetic coupling effects in multilayer films. Magnetic multilayer films have great potential for magnetic recording in computers In $3d/3d$ [69], $3d/4d$ [70] and in similar systems magneto resistance oscillations are observed. The oscillatory behaviour between ferromagnetic and antiferromagnetic coupling in $3d/3d$ system [68] and in $3d/4d$ systems [71] are also observed. Among those the combination of partially occupied *d*-level elements. (*T*) and completely filled *d*-level elements (*B*) form an intermetallic binary compounds, satisfying the Daltons law of definite proportions according to which the numerical subscripts attached to the symbols for the elements in chemical formulae must be integers [72,73]. These combinations of TB, TT or BB formed with elements give rise to series of compounds, some of which have complicated indices in their chemical formulae and some having simple indices. Most of the series of compounds of TB and I_BB obey the rules governing the electron concentration per atom [74], where the classification of elements such as T, B and I_B has been done by Pauling [75] on the basis of

the scheme for different energy levels which may be occupied by electrons around a nucleus as shown in Figure 7. Figure 7 shows that the energy of the 3*d* level is intermediate

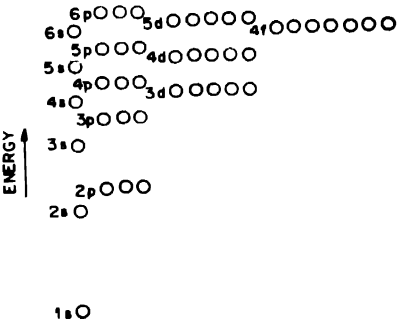

Figure 7. Approximate scheme for the stability of electron levels

between those of the 4*s* levels and 4*p* levels, with consequently a very large number of possible electron exchanges and hybrid bonding orbitals . *d-s*, *d-p* and *d-s-p*. To clarify this complicated situation, it is essential to have to its fullest extent, the information provided by the study of the magnetic properties of these compounds

For compounds with unpaired electrons, we can distinguish two regions on either side of a transition temperature : the coupling region at low temperatures where there are ferromagnetic or antiferromagnetic interactions between the spins of these electrons, and the paramagnetic region at high temperature where these interactions are destroyed by thermal agitation. The transition point (the Curie or Neel point) is often referred to as the coupling temperature T_c. The temperature variation of the molar magnetic susceptibility (the product of the susceptibility and the sum of the atomic weights of the different atoms including one magnetic atom) readily allows one to recognize these regions, shown in Figure 8. In the paramagnetic region, the molar susceptibility satisfied a simple law, the so-called Curie-Weiss law. The Langevin theory of paramagnetism, together with the Weiss

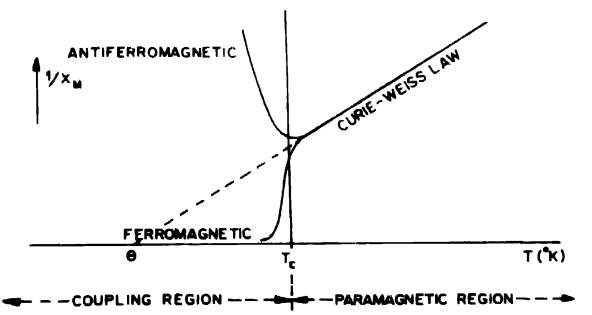

Figure 8. Magnetic coupling and the Curie-Weiss law.

theory, in which the orbital moments (due to the orbiting of the electrons around the nucleus) and the spin moments (due to the intrinsic moment of the electrons themselves) of

several electrons are coupled to one another to form the resultant moment of the atom For weak magnetic fields, which do not disturb this coupling, the electron has angular momentum for which azimuthal quantum number (l) and electron spin quantum number equal to 1/2. The most important mode of coupling is known as Russell-Saunders and in it the l and s are coupled strongly as explained in Ref. [69].

Important scientific aspects of the study of the electronic properties of artificial metallic superlattices or multilayers will continue to involve 2D–3D dimensional crossover phenomena (transport, magnetic, superconduction), the stabilization of metastable compounds (through heteroepitaxy), interlayer coupling effects (exchange or dipole magnetic coupling, Josephson superconducting tunneling, activated classical or quantum mechanical normal electron tunneling *etc*). The ability to turn on the 3D by adjusting the interlayer coupling in insulator/metal superlattices is only begining to be appreciated

The important point for d-band transition metals is that in surface orientations of monolayers of these materials, the magnetic moment is enhanced as compared to bulk values, as has been observed experimentally [76]. The reason for this behaviour is directly related to the particular shape of the local DOS rather than to the narrowing of the band due to the decrease of the coordination number. These local DOS are quite different from the ones in the bulk to those of surface orientation of monolayers or bilayers [77]. The recent most interesting development in the field of Fe based multilayer ultrathin magnetic films is that the observation of antiferromagnetic coupling of Fe films in Fe/Cu/Fe [64] and Fe/Cr/Fe [78,79] sandwitches and multilayers respectively. This system actually displays oscillatory Fe-Fe coupling, changing from ferromagnetic to antiferromagnetic and back again as the number of Cr [79]/Cu [69] layers increases. Ultrathin magnetic superlattices and multilayers with alternate layers of magnetic and non-magnetic metals have profound potential in magnetic recording applications and are interesting for understanding physics of thin film magnetism, magnetics *etc* [80].

The ability to tailor magnetic anisotropy of a multilayer maintaing an overall (total) film thickness sufficient enough to generate a measurable signal, is an extraordinary advantage over a thin film magnetic recording head. Magnetic multilayers where the magnetic properties of the individual sublayers are varied could lead to multibit storage at a given site, the number of layers flipped could be adjusted by the strength of the external magnetizing fields. When these structures with thickness suitable to behave as antiferromagnetically coupled layers are subjected to magnetic field in the plane parallel to the interfaces, a critical field is observed at which the alignment of spins in the magnetic film [81].

It is found in ultrathin films of *fcc*-Fe/Cu(111) that the easy axis is normal to the film plane Such perpendicular anisotropy is reported by Kummerle and Gradmann [38] on *fcc*-Fe/Cu(111). SMOKE characterisation of *fcc*-Fe/Cu(100) [82] shows that unlike conventional magnetic systems where the magnetization increases with the decrease in temperatures in case of *fcc*-Fe/Cu(100), the ferromagnetism disappears on cooling the

sample to room temperature as shown in Figure 9. As a consequence, the sticking coefficient of the Fe on Cu is very different for depositions made for ferromagnetic and non-ferromagnetic states. Another intriguing feature of the SMOKE signal is that the hysterisis curve is always of the same height, independent of Fe thickness (from 1-10 monolayers). The Fe films on the different Cu single crystal substrates, all show the same characteristic behaviour despite having different structures (*fcc* and *bcc*) and different interface symmetries. As shown in Figure 10, the dramatic drop in perpendicular remanence

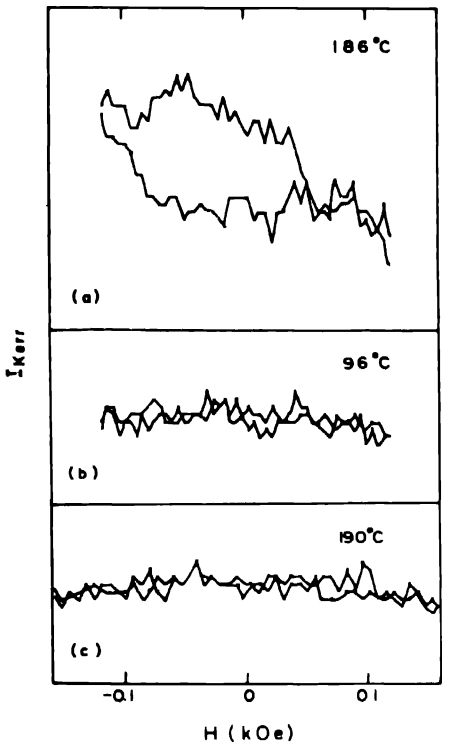

Figure 9. SMOKE signals are shown for three atomic layers of (1×1) Fe/Cu(100). The ferromagnetic signal in (a), for a film grown and measured at ~ 190°C, corresponds to that from a monolayer, based on the Fe/Au(100) calibration. Panels (b) and (c) show that the signal disappears on cooling and does not reappear upon reheating.

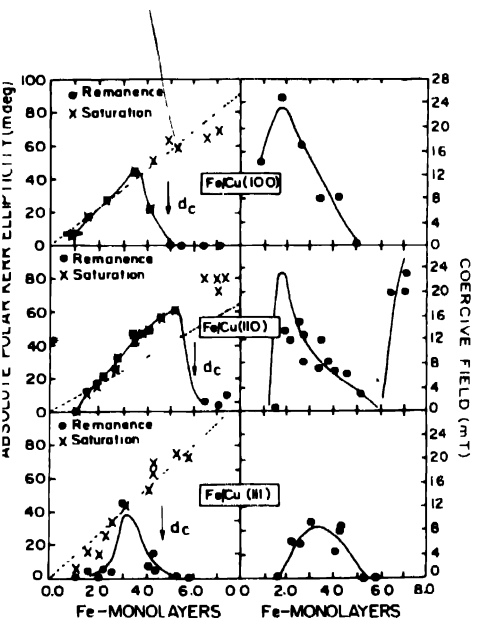

Figure 10. Absolute polar Kerr ellipticity (left) and coercive field (right) for ultrathin films of Fe grown at 80 K on Cu(100), Cu(110) and Cu(111) as a function of Fe thickness. The solid lines indicate the general trend of the Kerr remanence and coercive field. Films thicker than 6.5 ML may not be saturated by the 560 mT applied field. Note the similar behaviours for all three systems which have a critical thickness d_c between 4.5 and 6 ML at which the magnetization changes orientation from perpendicular to in-plane. Note that on Cu(111) only the 3-ML Fe films exhibited a square hysteresis loop as deposited at 80 K, however several other Fe films exhibited a square loops as well after annealing to room temperature. The dotted lines show predictions for the Kerr ellipticity based upon numerical simulations.

and coercive field with increasing thickness, the Fe films grown on Cu(100), Cu(110) and Cu(111) all display a perpendicular easy axis with a critical thickness d_c between 4.5 and 6

ML [42]. Fe/Pd/Fe trilayers [83,84] or multilayers [38,82,85] are attractive materials because of their important properties. A large perpendicular anisotropy with high coercive force [38] and a large Kerr rotation effect [82] are obtained and these multilayer films can be used in high density magneto-optical recording medium [86].

The *fcc*-Fe deposited at elevated temperatures, goes into a metastable ferromagnetic state. This state is believed to be associated with an expanded interlayer spacing. The existence of a surface structure phase transition at these temperatures in deserving of further investigation from the point of view of catalysis [82].

The giant magnetoresistance (GMR) effect is first discovered by Baibich *et al* [83] for Fe/Cr multilayers. This discovery has generated an enormous interest in the field of metallic superlattices in general, in the basic mechanism responsible for the effect [87] and possible magnetoresistive applications. Later, a large negative GMR for currents in the plane of the layers is found in Fe/Cr multilayers [88]. Parkin *et al* [89] have subsequently found oscillations both in the MR ratio and in an exchange coupling energy between magnetic layers as a function of non-magnetic spacer layer thickness, which is directly related to the origin of the GMR. Since then considerable combinations of ferromagnetic/non-ferromagnetic multilayers [90,91(a)] have been reported (see Figure 11 for oscillation of MR ratio as a function of thickness of Cu) to show the GMR effect and

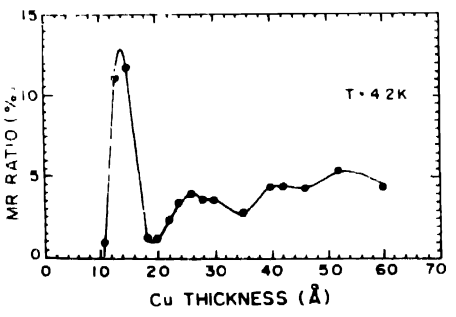

Figure 11. Variation of the magnetoresistance (MR) ratio as a function of the thickness of copper (Cu for 60×(15-Å Fe/Cu Cu) multilayers. The solid line is a guide for the eye.

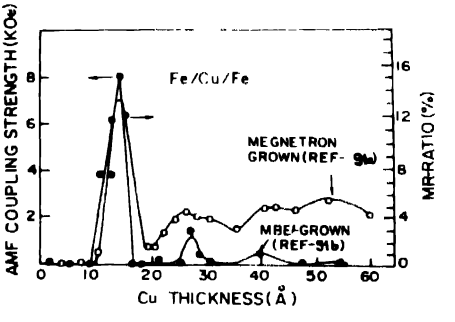

Figure 12. Comparison of the oscillations in AFM-coupling strength for MBE-grown Fe/Cu/Fe multilayers on Cu(100) from Ref. [91(b)] and the oscillations in the magnetoresistance ratio for magnetron-grown, (111) textured Fe/Cu/Fe multilayers from Ref. [91(a)].

oscillatory behaviour of the exchange coupling strength. Recent publications have demonstrated the existance of oscillatory antiferromagnetic (AFM) exchange coupling as a function of Cu spacer-layer thickness in Fe/Cu/Fe [91(a), 91(b)] as shown in Figure 12. There has been great interest in the GMR of metallic magnetic multilayers of a ferromagnetic film alternated with a non magnetic film.

For a better understanding of the GMR effect, it is important to characterize the conduction electron scattering by the simultaneous measurement of other electrical transport properties. In fact until now, thermoelectric power [65,92,93] thermal

conductivity [94] and Hall effect [95,96] measurements on multilayer systems have been undertaken. Sato *et al* [96] have found an anomalous field dependence of Hall resistivity for an Fe/Cr multilayers with a large MR and explained the dependence as a reduction of left-right asymmetric conduction electron scattering correlated with the GMR [96]. It is of interest to know whether it is a common character of multilayers exhibiting GMR.

6. Wedge shaped Fe films

Fe wedges on Cu(100) can be studied similar as above but the lattice matching permits *fcc* and tetragonally distorted *fcc* phases to provide structural complexity in addition to the interplay of competing magnetic anisotropies. A spin reorientation transition can thus be studied in the center of the wedge where the competing anisotropies cancel as shown in Figure 13 [97].

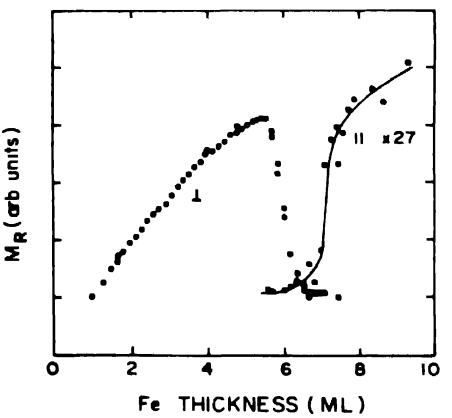

Figure 13. Spin reorientation transition for Fe/Cu(100) in wedge shaped sample

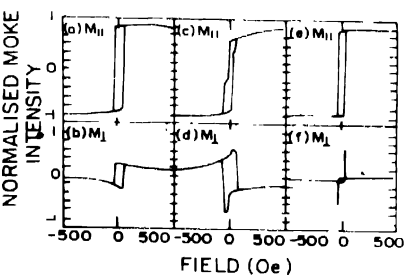

Figure 14. Typical MOKE loops for the Fe wedged film for r=0.4±0.02 (a) M_{II}-H and (b) $M_{\perp}$-H loops at Φ = 75° (c) M_{II}-H and (d) $M_{\perp}$-H loops at Φ = 20° (e) M_{II}-H and (f) $M_{\perp}$-H loops at Φ = 60°

For the fixed thickness films the values of the anisotropy constants are accurately determined by Brillouin light scattering (BLS) measurements together with polar magneto-optic Kerr effect (MOKE) measurements that gave the value of the magnetization The wedge shaped Fe film on GaAs(001) for an anisotropy ratio $r = 0.4 \pm 0.02$ shows three typical sets of MOKE loops (Figure 14) illustrating the different switching behaviours as a function of the angle between the applied field and the in-plane crystallographic axes [98] Figures 1(a) and 1(b) show $M_{\|}$ -H and $M_{\perp}$ -H loops respectively, for Φ = 75°. Both loops show one irresversible jump at the same field of ~ 50 Oe as the field is reversed corresponding to 'one-jump' switching. Figures 1(c) and 1(d) show $M_{\|}$ -H and $M_{\perp}$ -H loops respectively, for Φ = 20°. Here both loops show two irreversible jumps as the field is reversed, corresponding to 'two jump' switching. These two jumps, each occur when the magnetization traverses each of the two hard axis directions that exist in a sample with $|r| < 1$. This implies that when the uniaxial anisotropy dominates over the cubic anisotropy

(*i.e.* $|h| > 1$), only one-jump switching should occur, and this behaviour is indeed observed. Figures 1(e) and 1(f) show $M_{\parallel}$ -H and $M_{\perp}$ -H loops, respectively, for $\Phi = 60°$. In this case, a 'reversed' two jump switch occurs since the magnetization initially rotates away from the field direction in a clockwise sense, say, but switches back over the field direction in an anticlockwise sense.

7. Conclusions

Ultrathin films of transition metals, such as iron, have been found interesting for growth, orientation and surface properties. We have given all possible defects prevalent and the models of deposition in such case. A brief review of properties are presented to signify the importance of such systems of monolayers. In the end, peculiarties of wedge shaped Fe films are also described.

Acknowledgment

We are grateful to Prof E S R Gopal, Director NPL for keen interest and for permission to publish this work. One of the authors (GSNR) is thankful to the Council of Scientific and Industrial Research for granting Pool officership to him to complete this work.

References

[1] R W Cahn, P Haasen and E J Kramer *in the "Material Science and Technology/processing of metals and alloys* ed R W Cahn **Vol. 15** p 289 (1991) , Donald W Pashley *Adv. Phys* **5** 173 (1956)

[2] G Honjo and K Yagi *in Current Topics in Material Science* **Vol. 6** (Amsterdam North Holland) p 195 (1980)

[3] R Vincent *Phil. Mag* **19** 1127 (1969)

[4] K Yakayanagi, K Yagi, K Kobayashi and G Honjo *J Cryst Growth* **28** 243 (1975)

[5] Y Kuk, L C Feldman and P J Silverman *Phys Rev Lett* **50** 511 (1983)

[6] G I Finch and A G Quarrell (a) *Proc Roy. Soc* A141 398 (1933) , (b) *Proc Phys Soc (London)* **46** 148 (1934)

[7] N A Shishakov *Zh Eksper Teor Fiz* **22** 241 (1952)

[8] R C Newman *Proc Phys Soc* **B69** 432 (1956)

[9] W Cochrane *Proc Phys Soc* **48** 723 (1936)

[10] F C Frank and J H van der Merwe (a) *Proc Roy Soc* **A198** 95 (1949), (b) *Proc Roy Soc* **A200** 125 (1949); (c) *Proc Roy Soc* **A201** 261 (1950)

[11] J H van der Merwe *J. Appl Phys* **34** 117 (1963), *J Appl. Phys* **34** 123 (1963)

[12] W A Jesser and D Kuhlmann-wils-dorf *Phys Stat Solidi* **19** 95 (1967)

[13] G Honjo, K Takayanagi, K Kobayashi and K Yagi *J Crys Growth* **42** 98 (1977)

[14] (a) E Bauer and H Poppa *Thin Solid Films* **12** 167 (1972), (b) E Bauer (unpublished work)

[15] I Markov and S Stoyanov *Contemp Phys* **28** 267 (1987)

[16] E Bauer and J H Vander Merwe *Phys Rev* **B33** 3657 (1986)

[17] J A Venables and G L Price in *Epitaxial Growth* ed J W Mathews (New York Academic) p 382 (1975)

[18] J A Venables, G D T Spiller and M Hanbuchen *Rep Prog Phys* **47** 399 (1984)

[19] D Walton *Phil. Mag* **7** 1671 (1962)

[20] R Kern, G Le Lay and J J Metois in *Current Topics in Material Science* **Vol. 3** (Amsterdam : North Holland) p 131 (1979)

[21] N Osakabe, Y Fanishiro, K Yagi and G Honjo *Surf Sci.* **97** 393 (1980)

[22] J A Venables, J Derrien and A P Janssen *Surf Sci* **95** 411 (1980)

[23] L M Falicov *Thin Solid Films* **216** 169 (1992)

[24] A C Gossard *Molecular Beam Epitaxy of Superlattices in Thinfilms* (*Treatise on Material Science and Technology* **Vol. 24**) (New York Academic) Ch 2 (1982)

[25] (a) S M Durbin, J E Cunningham, M E Mochel and C P Flynn *J Phys F: Metal Phys.* **11** L223 (1981), (b) S M Durbin, J E Cunningham and C P Flynn *J Phys* **F12** L75 (1982)

[26] M J Pechan, J F Anknei, C F Majkrazk, D M Kelly and I K Schuller *J. Appl Phys* **75** 6178 (1994), J Q Zheng, J B Ketterson, C M Falco and I K Schuller *Physica* **B&C 108** 945 (1981); E E Fullerton, J E Mattson, S R Lee, C G Sowers, Y Y Huang, G Felcher, S D Bader and F T Parker *J Magn. Magn Mater* **117** L301 (1992), M R Khan, C S L Chan, G P Felcher, M Grimsditch, A Kuany, C M Falco and I K Schuller *Phys Rev* **B27** 7186 (1983), J E Mattson, S Kumar, E E Fullerton, S R Lee, C H Sowers, M Grimsdtch, S D Bader and F T Parker *Phys Rev Lett* **71** 185 (1993), J E Mattson, E E Fullerton, S Kumar, S R Lee, C H Sowers, M Grimsdtch, S D Bader and F T Parker *J. Appl Phys* **75** 6169 (1994)

[27] G Brauer and J Jander *Z Anorg Allg. Chem* **270** 10 (1952); G Brauer and R Esselborn *ibid* **309** 151 (1961), *ibid* **308** 53 (1961)

[28] E V Storms *High Temperature Science* **7** 103 (1975)

[29] I L Singer, S A Wolf, W H Lowrey and J S Murday *J Vac Sci Technol* **15** 625 (1978)

[30] I L Singer (Private Communication) (1978), J R Gavaler *IEEE Trans on Mag* **15** 623 (1979)

[31] R F Farrow, P W Sullivan, G M Williams, G R Jones and D C Camerson *J Vac Sci Technol* **19** 415 (1981), P W Sullivan, R F C Farrow and G R Jones *J Crys Growth* **60** 403 (1982)

[32] R Z Mezey and J Gilet *Jpn J Appl Phys* **21** 1569 (1982)

[33] M T Kief and W F Egelhoff (Jr) *J Vac Sci Technol* **A11** 1661 (1993)

[34] S D Healy, K R Heim, Z J Yang, G G Hembree, J S Drucker and M R Scheinfein *J Appl. Phys* **75** 5592 (1994)

[35] M T Kief and W F Egelhoff (Jr) *Phys Rev* **B47** 10785 (1993)

[36] G L Nyberg, M T Kief and W F Egelhoff (Jr) (unpublished)

[37] (a) U Gradmann, W Kummerle and P Tillmanns *Thin Solid Films* **34** 249 (1976), (b) W Kummerle and U Gradmann *Solid State Commun* **24** 33 (1977)

[38] W Kummerle and U Gradmann *Phys Stat Solidi* **A45** 171 (1978)

[39] (a) C Rau, C Schneider, G Xing and K Kamison *Phys Rev Lett* **57** 3221 (1986), (b) Y Darici, J Marcano, H Min and P A Montano *Surf Sci* **195** 566 (1988)

[40] D Tian, F Jona and P M Marcus *Phys Rev* **B45** 11216 (1992)

[41] S A Chambers, T J Wagener and J H Weaver *Phys. Rev* **B36** 8992 (1987)

[42] M T Kief and W F Egelhoff (Jr) *J Appl Phys* **73** 6195 (1993)

[43] C Liu and S D Bader *J Vac Sci Technol* **A8** 2727 (1990); U Scheithauer, G Meyer and M Henzler *Surf Sci* **178** 441 (1986)

[44] Q Jiang, Y L He and G C Wang *Surf Sci* **295** 197 (1993)

[45] S A Chambers, F Xu, H W Chen, I M Ustomirov, S B Anderson and J H Weaver *Phys. Rev.* **B34** 6605 (1986)

[46] G C Smith, H A Padmore and C Norris *Surf. Sci. Lett* **119** L287 (1982)

[47] K E Johnson, D D Chambliss, R J Wilson and S Chiang *J. Vac. Sci. Technol.* **A11** 1654 (1993)

[48] W A Jesser and J W Matthews *Phil Mag* **15** 1097 (1967)

[49] Y L He and G C Wang *Phys Rev Lett* **71** 3834 (1993)

[50] G A Prinz and J J Krebs *Appl. Phys. Lett.* **39** 397 (1981)

[51] N C Koon, B T Jonker, F A Volkening, J J Krebs and G A Prinz *Phys. Rev Lett* **59** 2463 (1987)

[52] R Richter, J G Gay and J R Smith *Phys Rev Lett.* **54** 2704 (1985) and *J. Vac. Sci. Technol.* **A3** 1498 (1985)

[53] C L Fu, A J Freeman and T Oguchi *Phys Rev. Lett* **54** 2700 (1985)

[54] M F Onellion, C L Fu, M A Thompson, J L Errkine and A J Freeman *Phys. Rev.* **B33** 7322 (1986), J P Bibariain and G A Somorjai *J. Vac. Sci. Technol* **26** 2073 (1979), S D Badai *Proc. IEEE* **78** 909 (1990); G A Prinz *J. Magn. Magn' Mater.* **100** 469 (1991)

[55] W A Jesser and J W Matthews *Phil. Mag.* **17** 595 (1968), H J G Dreatsma, H M van Noort and F J A den Broeder *Thin Solid Films* **126** 117 (1985), M Kato, S Fukase, A Sato and T Mori *Acta Metall.* **34** 1179 (1986); Y Ando and D J Dingley *Jpn. J. Appl. Phys.* **29** 939 (1990), K E Johnson, D D Chambliss, R J Wilson and S Chiang *J. Vac. Sci. Technol* **A11** 1654 (1993)

[56] H Li and B P Tonner *Phys. Rev.* **B40** 10241 (1989), *Surf. Sci* **237** 141 (1990)

[57] M T Kief and W F Egelhoff (Jr) *J. Vac. Sci. Technol.* **A11** 1661 (1993)

[58] U Gradmann and P Tillmanns *Phys. Stat. Sol* **A44** 539 (1977)

[59] F Pontkess and H Nedermayer *Physica* **B161** 276 (1989)

[60] J W Evans *Phys. Rev* **B39** 5655 (1989), D E Sanders and J W Evans in *The Structure of Surfaces III* p 380 (Berlin : Springer-Verlag) (1991)

[61] D Tian, H Li, F Jona and P M Marcus *S. S. Commun* **80** 783 (1991), S Andrieu, M Piecuch and J Bobo *Phys. Rev* **B46** 4909 (1992)

[62] J Thomassen, B Feldman and M Wuttig *Surf. Sci* **264** 406 (1992)

[63] W Doum, C Stuhlmann and H Ibach *Phys. Rev. Lett* **60** 2741 (1988)

[64] B Heinrich, Z Celinski, J F Cochran, W B Muir, J Rudd, Q M Zong, A S Arrott, M Myrtle and J Kirschner *Phys. Rev. Lett* **64** 673 (1990)

[65] M J Conover, M B Brodsky, J E Mattson, C H Sowers and S D Bader *J. Magn. Magn. Mater* **102** 15 (1992)

[66] J Tomassen, F May, B Feldmann, M Wuttig and H Ibach *Phys. Rev. Lett* **69** 3831 (1992)

[67] L Gonzalez, R Miranda, M Salmeron, J A Vergas and F Yndurain *Phys. Rev* **B24** 3245 (1981)

[68] S O Demokritov, J A Wolf and P Grunberg *Appl. Phys. Lett* **63** 2147 (1993)

[69] Eric E Fullerton, M J Conover, J E Mattson, C H Sowers and S D Bader *Phys. Rev* **B48** 15755 (1993)

[70] S S P Parkin, N More and K P Roche *Phys. Rev. Lett* **64** 2304 (1990)

[71] Z Q Qiu, J Pearson, A Berger and S D Bader *Phys. Rev. Lett* **68** 1398 (1992), Z Q Qiu, J Pearson and S D Bader *J. Appl. Phys* **73** 5765 (1993), D T Pierce *Bull. Am. Phys. Soc* **37** 196 (1992), M Johnson, S T Purcell, NWE McGee, P Cochoorn, J ann de Stegge and W Hoving *Phys. Rev. Lett* **68** 2688 (1992), J E Mattson, E E Fullerton, C H Sowers, Y Y Huang, G P Fecher and S D Bader *J. Appl. Phys* **73** 5969 (1993)

[72] E Zintl, J Goubeau and WZ Dullen Kopf *Phys. Chem* **A154** 1 (1931)

[73] E Zintl and H Z Kaiser *Anorg. Chem* **211** 113 (1933)

[74] W Hume-Rothery *The Structure of Metals and Alloys (Inst. Metals, London)* (1936)

[75] L C Pauling *The Nature of Chemical Bond* (Cornell, Ithaca) (1960)

[76] L M Falicov, D T Pierce, S D Bader, R Gronsky, Kristl B Hathaway, H J Hopster, D N Lambeth, S S P Parkin, G Prinz, M Salamon, I K Schuller and R H Victora *J. Mater. Res.* **5** 1299 (1990)

[77] Z Celinski, B Heinrich, J F Cochran, W B Muir, A S Arrott and J Kirschner *Phys. Rev. Lett* **65** 1156 (1990)

[78] P Grunberg, R Schreiber, Y Pang, M B Brodsky and H Sowers *Phys. Rev. Lett* **57** 2442 (1986), C Carbone and S F alvarado *Phys. Rev* **B36** 2433 (1987), Van Dan, A Fert, P Etienne, M N Baibich, J M Broto, J Chezelas, G Crenzet, A Friederich, S Hadjoudj, H Hurdequint, J P Recloules and J Massies *J. Phys. (Paris) Colloq* **49** C-8-1633 (1988)

[79] J J Krebs, P Lubitz, A Chaiken and G A Prinz *J. Appl. Phys* **67** 5920 (1990)

[80] L M Falicov *Phys. Today* **45** 46 (1992), R L White *IEEE Trans. Magn* **28** 2482 (1992)

[81] J R Cullen and K B Hathaway *Phys. Rev.* **B47** 14998 (1993)

[82] E R Moog, S D Bader, P A Montano, G Zajac and TH Fleisch *Superlattices and Microstructures* **3** 435 (1987)

[83] M N Baibich, J M Broto, A Fert, F Nguyen van Dau, R Petroff, P Etienne, G Creuzet, A Friederich and J Chazel *Phys. Rev. Lett.* **61** 2472 (1988)

[84] A Boufelfel, M Roy, Emrick Charles and M Falco *Phys. Rev.* **B43** 13152 (1991)

[85] P M Levy, K Ounadjela, S Zhang, Y Wang, C B Sommers and A Fert *J. Appl. Phys.* **67** 5914 (1990)

[86] U Gradmann *J. Magn Magn. Mater* **54-57** 733 (1988); J A O'Sullivan, D G Porter, R S Indeck and M W Muller *J. Appl. Phys* **75** 5753 (1994)

[87] P M Levy *Solid State Physics* **Vol. 47** eds. D Turnbull and H Ehrenreich (San Diego : Academic) (in press) (1994); A Fert and P Bruno *Ultra Thin Magnetic Structure* eds. B Heinrich and A Bland (Berlin : Springer-Verleg) (in press)

[88] G Binasch, P Grunberg, F Saurenbach and W Zinn *Phys. Rev.* **B39** 4828 (1989)

[89] S S P Parkin, N More and K P Roche *Phys. Rev. Lett.* **64** 2304 (1990)

[90] T Shinjo and H Yamamoto *J. Phys. Soc. Jpn.* **59** 3061 (1990); F Petroff, A Barthelemy, D H Mosca, D K Lottis, A Fert, P A Schroeder, W P Jr Pratt, R Laloee and S Lequien *Phys. Rev.* **B44** 5355 (1991); J E Mattson, C H Sowers, A Berger and S D Bader *Phys. Rev. Lett.* **68** 3252 (1992); S S P Parkin, R Bhadra and K P Roche *Phys. Rev. Lett* **66** 2152 (1991)

[91] (a) D H Mosca, F Petroff, A Fert, P A Schroeder, W P Pratt and R Laloee *J. Magn. Magn. Mater.* **94** L1 (1991); F Petroff, A Berthelemy, D H Mosca, D K Lottis, A Fert, P A Schroder, W P Pratt (Jr) and R Loloee *Phys. Rev.* **B44** 5355 (1991); (b) W R Bennett, W Schwarzacher and W F Egelhoff (Jr) *Phys. Rev. Lett.* **65** 3169 (1990)

[92] J Sakurai, M Horie, S Araki, H Yamamoto and T Shinjo *J. Phys. Soc. Jpn.* **60** 2522 (1991)

[93] L Piraux, A Fert, P A Schroeder, R Loloee and P Etienne *J Magn. Magn. Mater.* **110** L247 (1992)

[94] H Sato, Y Aoki, Y Kobayashi, H Yamamoto and T Shinjo *J. Phys. Soc. Jpn.* **62** 431 (1993)

[95] S N Song, C Sellers and J B Ketterson *Appl. Phys Lett.* **59** 479 (1991)

[96] H Sato, T Kumauo, Y Aoki, T Kaneko and R Yamamoto *J. Phys. Soc. Jpn.* **62** 479 (1993)

[97] S D Bader, Donggi Li and Z Q Qiu *J. Appl. Phys.* **76** 6419 (1994)

[98] C Daboo, R J Hicken, D E P Eley, M Gester, S J Gray, A J R Ives and J A C Bland *J. Appl. Phys.* **75** 5586 (1994)

About the Reviewer

G S N Reddy : Dr. Reddy, Pool Officer, National Physical Laboratory, New Delhi, was born on December 2, 1955. He earned his BSc and MSc degrees at Sri Venkateswara University, in 1979 and 1981 respectively. He had his doctoral degree in theoretical solid state physics from Indian Institute of Technology, Delhi in 1987. For last eight years he has worked at NPL on high temperature Superconducting Quantum Interference Device (SQUID) and in superconductivity in general. For last two years his interest is concentrated in synthesis of metallic monolayers. He has about 40 publications in all including those in conferences.

V S Tomar : Dr. Tomar, a senior scientist in National Physical Laboratory, New Delhi, did his MSc (Physics) in 1963 from Vikram University and his PhD (Solid State Physics) in 1970 from University of Saugar. He did his post doctoral work in low temperature physics and superconductivity in Indian Institute of Technology, Kanpur for three years and in Swiss Federal Institute of Technology (ETH), Switzerland for three years. He joined NPL, New Delhi in 1974 as a Scientist and since then he has worked on Josephson Volt Standard, Superconducting Quantum Interference Device (SQUID) and on synthesis of superconducting thin films of low and high T_c superconductors. For last three years his interests are extended to surface science (Auger Spectroscopy) and in growth of metallic monolayers. He has about 100 publications to his credit.